Analysis of the influence of foundation compressibility on the behaviour of reinforced soil walls using PIV

Ezzein, F.[1], Bathurst, R.J.[1] and Take, W.A.[2]
[1]*GeoEngineering Centre at Queen's-RMC, Civil Engineering Department, Royal Military College of Canada, Kingston, Ontario, Canada*
[2]*GeoEngineering Centre at Queen's-RMC, Department of Civil Engineering, Queen's University, Kingston, Ontario, Canada*

ABSTRACT
In a previous paper by Ezzein and Bathurst (2008) the performance of two reduced-scale reinforced soil walls was reported. The two walls were nominally identical but with different foundation stiffness. The control wall was constructed over a rigid foundation. The second wall was constructed over a compressible foundation. Both walls were uniform surcharged in stages following construction. Quantitative differences between the two structures were detected using conventional contact-type instrumentation. In this paper the focus is on the use of a digital imaging technology called Particle Image Velocimetry (PIV) that was employed to measure wall facing and backfill soil displacements. PIV is demonstrated to provide accurate and more comprehensive measurements of facing deformations and foundation settlements. The PIV technique allowed continuous soil displacement and strain fields to be computed that were previously unavailable using contact-type instrumentation. These data provide a better understanding of wall performance including identification and location of the onset of internal shear bands in the reinforced soil zone and soil arching between the back of the wall face and foundation.

RÉSUMÉ
Dans un article précédent par Ezzein et Bathurst (2008), la performance de deux murs renforcés à échelle réduite fût rapportée. Les deux murs étaient identiques mais avec des fondations de rigidités différentes. Le mur contrôle a été construit sur une fondation rigide. Le second mur a été construit sur une fondation compressible. Les deux murs ont été surchargés uniformément en étapes, suite à la construction. Des différences quantitatives entre les deux structures ont été détectées à l'aide d'instrumentation conventionnelle de type contact. Le présent article est axé sur l'usage d'une technologie d'imagerie numérique, la vélocimétrie d'image de particules (PIV), qui a été utilisée pour mesurer les déplacements du parement et du remblai. Il a été démontré que la technique PIV donne des mesures exactes et plus complètes des déformations du parement et des tassements des fondations. La technique PIV a permis le calcul de champs continus de déformations et déplacements de sol qui n'étaient pas disponibles jusqu'à ce jour avec les instruments de type contact. Ces données fournissent une meilleure compréhension de la performance des murs, incluant l'identification et la localisation de la genèse des bandes de cisaillement interne dans la zone de sol renforcé et l'effet de voute dans le sol entre l'arrière du parement et la fondation.

1 INTRODUCTION

Geosynthetic reinforced soil retaining walls are now a mature technology since their introduction in the late 1970s and early 1980s. Their popularity is largely due to their cost effectiveness and ease of construction. However, current approaches for internal stability design simply assume that the wall is seated over a rigid (or very stiff) foundation (e.g. AASHTO 2007; CFEM 2006; NCMA 1997). Hence, they ignore the influence of foundation stiffness (compressibility) on the magnitude and distribution of reinforcement loads under serviceability and ultimate (collapse) conditions.

The effect of foundation and toe condition was recently investigated by Ezzein and Bathurst (2006, 2007, and 2008) using a series of reduced-scale model reinforced soil retaining walls. The response of these walls was compared to a control wall with rigid toe and foundation conditions to quantify the influence of horizontal, vertical toe restraint and foundation stiffness on the overall wall response. This paper is a continuation of this previous work in which the influence of foundation stiffness was investigated by constructing and surcharge loading two nominally identical walls (Wall 16 and 17) with different foundation stiffness (Ezzein and Bathurst 2008).

The difference between the current paper and previous papers is that this paper reports for the first time the use of the Particle Image Velocimetry (PIV) technique described by White et al. (2003) to record the deformations of the wall facing and backfill soil in these tests using sequential digital images.

Before the PIV methodology can be described in the context of this paper, it is necessary to first describe the general model wall test arrangement and methodology. Further details of the two walls described below can be found in the paper by Ezzein and Bathurst (2008).

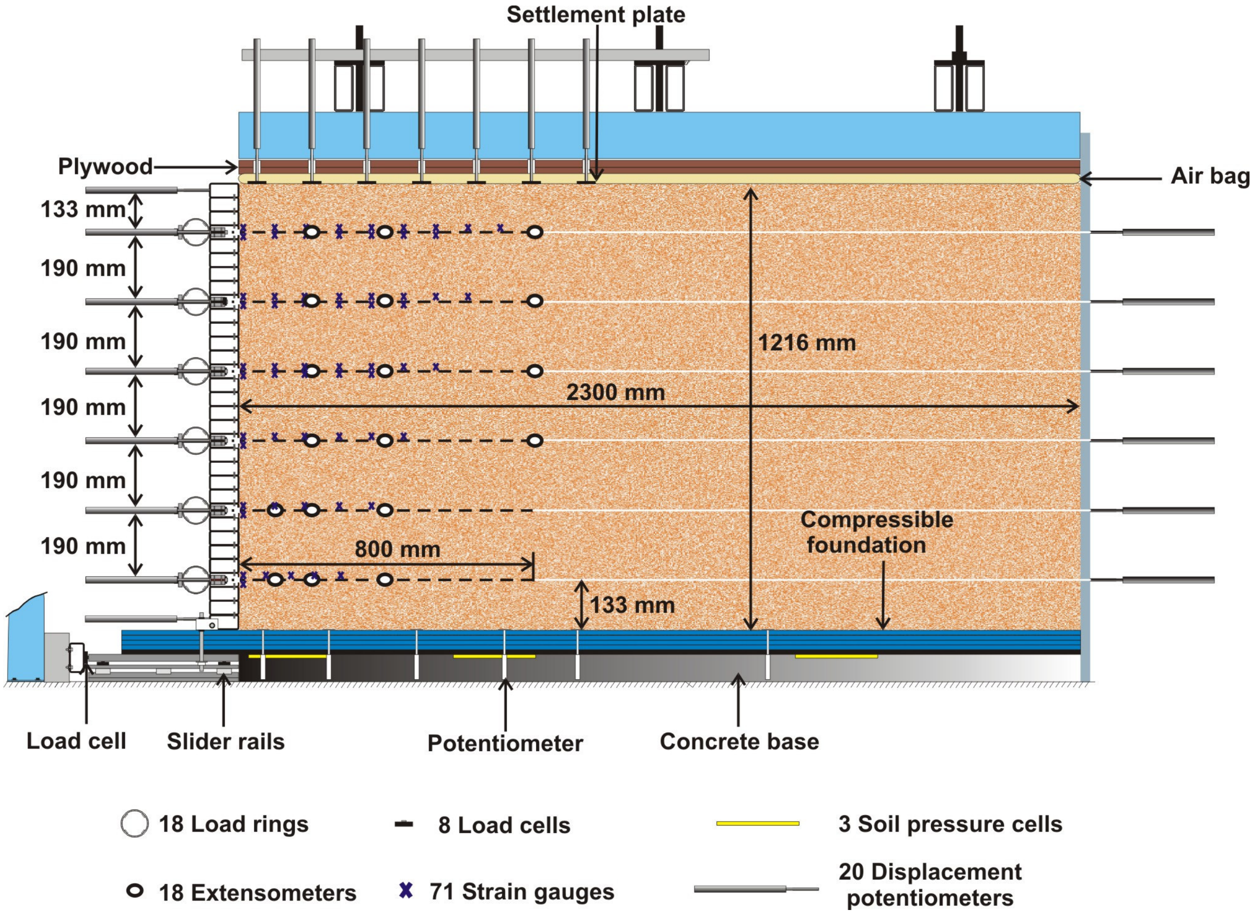

Figure 1. Cross-section view of model wall and instrumentation (Wall 17 with compressible foundation).

2 EXPERIMENTAL APPROACH

2.1 Test Facility and General Arrangement of Wall Models

The wall models were constructed in a specially designed strong box. A cross-section view of Wall 17 is shown in Figure 1. The walls were built to 1/6-scale with respect to prototype scale.

The inside dimensions of the strong box are 1.5 m high by 1.57 m wide by 2.91 m long. The base of the facility is seated on the laboratory concrete floor slab. The sidewalls of the test facility are comprised of transparent 18 mm-thick Plexiglas stiffened by an arrangement of steel braces. The combination of stiff external bracing, a model width to height ratio of 1.3 and sidewall friction reduction (using three layers of clear lubricated polypropylene sheets) resulted in boundary conditions approaching an idealized plane strain condition.

A uniform surcharge pressure was applied to the entire surface of the wall backfill using a pair of airbags restrained by two layers of plywood and reaction beams that are anchored to the strong floor using threaded rods.

The facing of the model walls was constructed from 32 stacked hollow structural steel sections (76 mm by 38 mm with a wall thickness of 4.8 mm). The sections were connected together by shear pins to transfer shear forces and to prevent lateral movement between section layers.

2.2 Materials

2.2.1 Soil Backfill

Clean uniform particle size rounded beach sand was selected as the backfill material in these tests. The same material has been used in the full-scale testing program at RMC (Bathurst et al. 2000, 2006) and in the earlier related work reported by Ezzein and Bathurst (2006, 2007 and 2008). The plane strain friction angle of the sand interpreted from laboratory plane strain tests is 44 degrees (Hatami and Bathurst 2005). The sand was placed in 190 mm lifts then compacted to bulk density of 1680 kg/m^3 using a hand plate tamper.

2.2.2 Reinforcement

Six layers of a commercially available knitted and coated polyester (PET) geogrid were used as the geosynthetic reinforcement material in this investigation and earlier related tests. The PET geogrid was modified by removing two out of three longitudinal members in order to achieve reasonable scaled tensile stiffness.

2.3 Toe and Foundation Condition

The objective of the current study was to investigate the influence of foundation compliance (stiffness) below both the facing and backfill on reinforced soil retaining wall performance. Two walls were constructed and tested that were identical except for the foundation boundary condition. Wall 16 was the control wall with the facing and backfill constructed on a rigid base (steel plate under facing and concrete base under the backfill). The toe of the wall was restrained horizontally and vertically. For the second wall (Wall 17), the entire model (facing and backfill) was constructed on compressible rubber and foam layers. The toe of Wall 17 was allowed to rotate and move vertically but was restrained in the horizontal direction by using a special hinge mechanism.

The rubber and foam materials, number of layers and their arrangement were selected based on numerical investigation (using FLAC models), standard correlations between subgrade modulus and soil type, and laboratory compression tests on candidate materials. The subgrade modulus stiffness value for Wall 17 is k_s = 1,840 kN/m^3. The vertical foundation stiffness in Wall 17 is equivalent to loose sand or very soft clay. For Wall 16 with a rigid toe, the value of k_s is assumed as infinity.

2.4 Wall Construction and Surcharging

The construction procedure started by placing the facing units bottom-up to the elevation of each reinforcement layer. The sand was placed and compacted using a hand-held plate tamper. Six modified polyester geogrid reinforcement layers with a length 0.8 m were placed in each wall. The wall facing was braced externally during construction and no horizontal load was carried by the restrained footing models during this stage. Following construction the air bag surcharging system was installed. Initial readings were taken and the external props removed (end of construction). Next, a series of constant surcharge pressure increments was applied to the backfill surface using the air bag arrangement. Each surcharge load increment was maintained for 24 hours, until the maximum surcharge of 66 kPa. After 96 hours, the wall was unloaded in five steps.

2.5 Instrumentation

2.5.1 Contact type

The wall models were heavily instrumented with up to 138 instruments as shown in Figure 1. The horizontal facing displacements were measured by a single column of displacement transducers (potentiometers) mounted against the centreline of the wall face at the reinforcement elevations and at the top of the test facility. A single displacement potentiometer was used to check for possible displacement at the wall toe. Displacement potentiometers were also attached to settlement plates across the surface of the soil backfill behind the front facing. The foundation settlement of Wall 17 was measured by five displacement potentiometers installed in the concrete base along a line perpendicular to the facing column. The cores of these devices were pointed upward and attached to settlement plates to record compression (settlement) of the compressible foundation layer.

Button load cells were installed at the footing to measure the vertical and horizontal toe reactions. Wire-line extensometers were attached to the reinforcement layers and monitored by displacement potentiometers mounted at the back of the test facility. Strain gauges were bonded to selected longitudinal members of each reinforcement layer. Load rings were used to measure connection loads between the facing wall and reinforcement layers. Finally, three earth pressure cells were embedded in the concrete foundation to record vertical earth pressure at the base of the test facility. The data from all instruments were recorded continuously using an HP 3497A data acquisition system controlled by a PC computer running HP VEE software.

2.5.2 PIV

The PIV technique combines three technologies: digital still photography, Particle Image Velocimetry (PIV) and close range photogrammetry:

- Digital still photography captures the arrangement of soil particles in an image matrix containing the intensity (brightness) recorded at each CCD (Charged Coupled Device) pixel;
- Particle Image Velocimetry (PIV) is a digital image correlation technique in which sub-regions of the image intensity matrix can be found in subsequent images to a high sub-pixel accuracy, thereby enabling vector displacements of the soil to be calculated between images, and;
- Close range photogrammetry enables the conversion of the coordinates of displacement data from units of pixels (image space) to units of mm (object space) while correcting for camera movements between images and camera lens distortion.

In this paper, the PIV technique is used for the first time to quantify wall facing and soil deformations that occurred between the end of construction and at selected times during and at the end of surcharging.

A Canon PowerShot G6 digital camera was used to remotely capture images of the wall face and soil at an image size of 3072×2304 pixels. The camera was mounted at a distance of 2.4 m from the north side of wall facility. The images were shot through the transparent Plexiglas wall and the lubricated polyethylene friction reducing membrane.

Since the precision of PIV is about 1/10th of a pixel (White et al. 2003) and the monitored area is relatively large, the field of view for each image had to be reduced and six separate images captured at each stage during the test program. At the photogrammetry step, the data from all six images was assembled and corrected for camera movements.

Prior to starting wall construction a total of 117 PIV control marks consisting of a black dot on a white background were drawn on the inside Plexiglas sheet of the north side of model test. The purpose of these control markers is to provide a minimum of 16 to 20 control markers in each field of view. The three layers of clear lubricated polypropylene sheets were placed over the Plexiglas to minimize sidewall friction while ensuring that the model wall and backfill remained visible.

3 PIV ANALYSIS

Digital photographs of the backfill sand and wall face were taken at intervals during the entire test and stored on a PC hard drive attached to the camera through a USB interface. These images were subsequently used for PIV analysis.

The initial image (prior to releasing props) was divided into a grid of 64 x 64 pixel square patches. At the focal length used to capture these images the size of a pixel corresponds to 0.23 mm in object space. Thus, the tracked patches correspond to 14.5 mm square regions of sand. The texture of each patch has unique information. In PIV, displacements are obtained by tracking the texture of each patch and then finding the location of the same patch in subsequent images. The change in patch location between images allows the movement vector to be computed in image space. The final calculation stage is to transform vectors in image space to vectors in engineering (object) space.

4 COMPARISON OF PIV MEASURMENTS AND CONTACT MEASUREMENTS

The displacements at the wall face and top of the soil backfill were monitored during surcharging by displacement transducers (potentiometers) mounted on the centreline of the test model and/or by manual survey. These conventional measurement methods provide an opportunity to compare the accuracy and consistency between measurement techniques. Figure 2 shows PIV measurements of the horizontal movement of the wall facing (Wall 16) versus measurements using manual survey. The comparison is made until some patches located over the top half of the wall face moved out of the camera field of view behind a strong box steel support column. Logarithmic axes are used for clarity particularly for low values of displacement. The vertical range bars in the plot correspond to maximum and minimum values deduced from target patches located in the vicinity of the manual survey points. The manual survey was carried out using a carpenter’s steel tape with an accuracy of ±1 mm. The open circles are best estimates. Over most of the data range the data points visually appear to plot closely around the 1:1 correspondence line. The exceptions are data points corresponding to manual survey readings less than 3 mm. To quantitatively examine the relationship between measurements more closely, the ratio (bias) of the PIV value to the corresponding (non-zero) manual reading was computed and the ratios plotted as shown in Figure 3. The data show that PIV readings are about 1.6 times greater than the manual readings for displacements less than about 3 mm. This is due to poor resolution of the manual tape reading. For displacements greater than 3 mm, both methods give similar values with a mean bias value of 1.01 and a coefficient of variation (COV) for bias values of 8.7%. The analysis of data in Figures 2 and 3 shows that displacement values using the PIV method

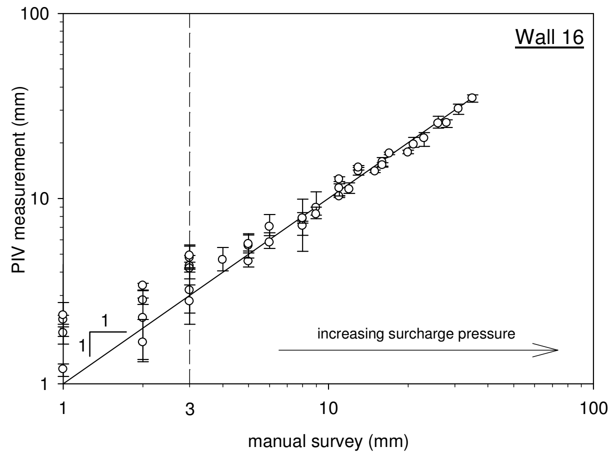

Figure 2. Outward facing displacements using PIV measurement versus manual survey measurements (Wall 16).

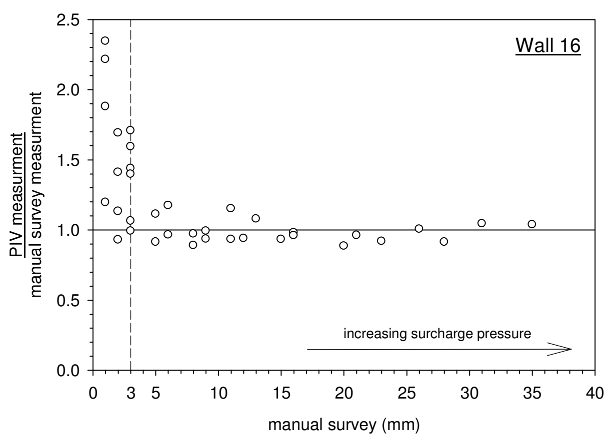

Figure 3. Ratio (bias) of PIV measurement versus manual survey measurement (Wall 16).

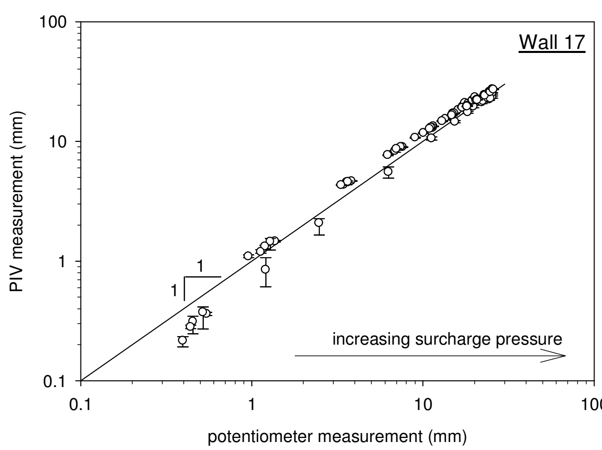

Figure 4. Foundation settlement using PIV measurements versus potentiometer (settlement plate) measurements (Wall 17).

are consistent with manual survey measurements when the manual survey values are sufficiently large. Below 3 mm of displacement, the PIV method is judged to be more accurate. However, it should be pointed out that the facing displacements in this investigation were tracked using the PIV method without improvement of the facing column cross-section texture which was viewed from the side. If this had been done, the range of displacements for each patch on the facing would be very much lower.

The top and the bottom boundaries of the soil backfill were visually obstructed by the horizontal steel sections supporting the strong box sidewalls. However, the PIV patches closest to the top and bottom of the backfill directly below and above contact measurement devices were tracked to measure the vertical displacement of backfill soil in the vicinity of these boundaries.

PIV measurements versus potentiometer readings of the compressible foundation settlement of Wall 17 are plotted in Figure 4. A similar comparison is shown in Figure 5 for the backfill surface settlement profile in Wall 16 from PIV measurements at a surcharge pressure of about 17 kPa. The plots show that both data sets are in reasonable visual agreement. However, there is a visually detectable over-estimation of vertical deformations near the bottom of the backfill using the PIV method for potentiometer readings greater than 1 mm (i.e. most data points fall above the 1:1 correspondence line in Figure 4). The mean and COV values of the ratio of PIV measurement to potentiometer measurement are 1.06 and 15.2%, respectively for potentiometer readings greater than 1 mm. On the other, the PIV measurements under-estimate soil surface settlement using settlement plates. There is a maximum discrepancy of 3 mm in Figure 5. The sources of discrepancy may be attributed to: a) the elevation of the measurement locations is not the same for each method; b) the PIV measurements are made at the lateral boundaries of the physical model while the contact measurements are made at the centreline; c) the wall facing does not move outward uniformly at each elevation, and; d) there may be distortions in soil movements at the vertical interface with the friction reducing polyethylene membrane and Plexiglas wall. The last three points imply that perfect idealized plane-strain boundary conditions in these tests may not have been achieved. However, from a practical point of view the physical test arrangement is judged to be as close to plane strain conditions as practical.

5 TEST RESULTS

An important advantage of the PIV technique over spot contact measurements is that continuous displacement and strain fields can be computed from images taken through the transparent sidewalls of the test facility. For brevity, only selected test results illustrating this advantage are presented here.

Figures 6 and 7 show the backfill displacement vector fields obtained using PIV for Walls 16 and 17 at q = 66 kPa surcharge pressure. It can be seen that the displacement of the backfill soil in Wall 17 with the compressible foundation support is greater than for Wall 16 constructed over a rigid support. The displacement component in the vertical direction contributes largely to

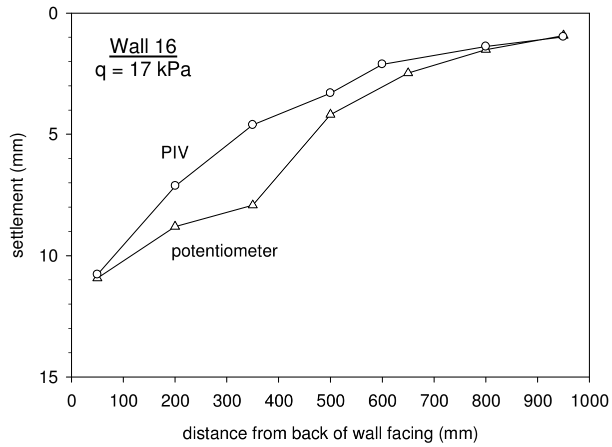

Figure 5. Backfill surface settlement using PIV measurements and potentiometer (settlement plate) measurements (Wall 16).

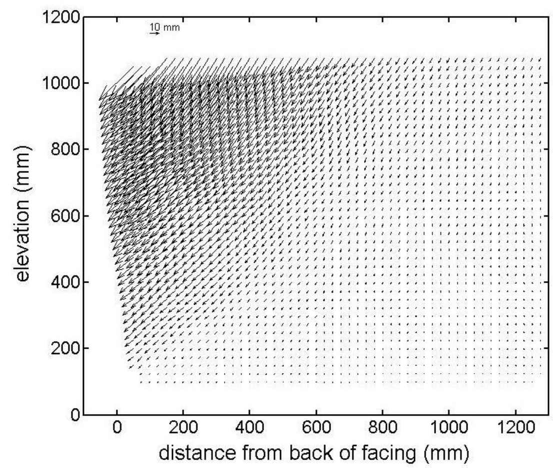

Figure 6. Backfill displacement vectors for Wall 16 (rigid base) at q = 66 kPa surcharge.

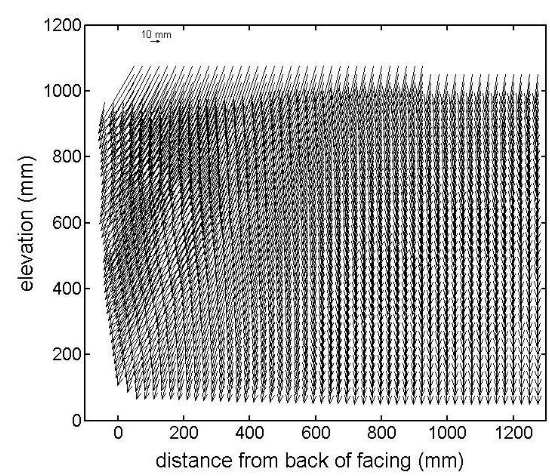

Figure 7. Backfill displacement vectors for Wall 17 (compressible base) at q = 66 kPa surcharge.

the greater overall soil displacements and outward facing deformations recorded for Wall 17. These results are consistent with horizontal facing measurements using manual survey and wall facing potentiometers reported by Ezzein and Bathurst (2008).

Displacement vector components can be presented as contour plots of backfill soil displacement. Vertical displacement component contour plots at maximum surcharge pressure for Walls 16 and 17 are shown in Figures 8 and 9, respectively. An interesting mechanism that is visible in Figure 9 is soil arching between the back of the wall facing and the foundation. This is generated by the soil directly behind the wall hanging up on the connections and load shedding to the facing column. Readings from potentiometer devices embedded in the foundation corroborate this interpretation as illustrated in Figure 10. As surcharge pressure increased the toe of the wall settled more and there is a pronounced reduction in compression of the compliant support layer at a distance of 20 to 720 mm behind the facing. At or beyond the reinforced soil zone (800 mm) settlement (or compression of the compliant base) is more uniform. This effect is also detectable in Figure 11 using vertical base pressures (σ_v) deduced from layer compression (i.e. compression of the foam support layer is proportional to vertical pressure with the foundation modulus determined from independent laboratory tests reported by Ezzein and Bathurst (2008)). In this figure, h is the height of structure above the base and γ is the unit weight of the facing column or soil. Local reduction in vertical earth pressure at the base of the backfill behind the facing column has been noted in full-scale reinforced soil walls constructed on a rigid foundation due to down-drag forces at the connections (Bathurst et al. 2000) and in earlier reduced-scale tests (Ezzein 2007).

In Figures 6 through 9 there are wedge-shaped zones that are consistent with the notion of an active soil wedge behind the facing. However, these are displacement vectors computed using the end of construction (prior to prop release) as the datum. Hence, the slopes deduced from the vectors or areas of constant colour do not correspond to the orientation of the Rankine active wedge. The location and extent of internal soil shear zones that are expected to occur after sufficient surcharge pressure were determined using PIV analysis. Contours of incremental shear strain are plotted in Figures 12 and 13 for Wall 16 and Wall 17, respectively. The strain increments are computed from displacements occurring between surcharge load stages (i.e. Δq). Contiguous shear zones are visually detectable in the figures and correspond to surcharge levels that resulted in the first occurrences of a well-defined soil failure. There are discontinuities in the contour distributions that are the result of the PIV algorithm attempting to interpolate across regions that are obscured by the strong box cross members (e.g. horizontal member at elevation about 550 mm and vertical members at about 475 and 950 mm from the back of the facing). The orientations of the these shear bands in the figures correspond roughly to the failure surface orientation predicted using Rankine earth pressure theory and the peak internal friction angle of the soil for this sand (ϕ = 44 degrees) previously reported by Hatami and Bathurst (2005). This is further evidence that

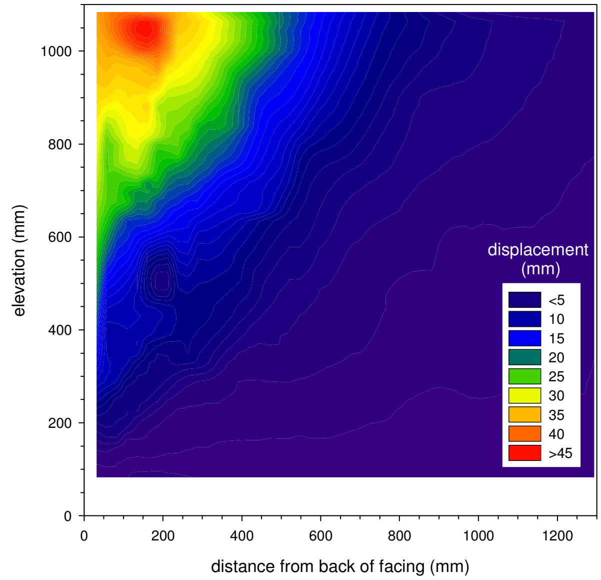

Figure 8. Vertical displacement contours for Wall 16 (rigid base) at q = 66 kPa surcharge.

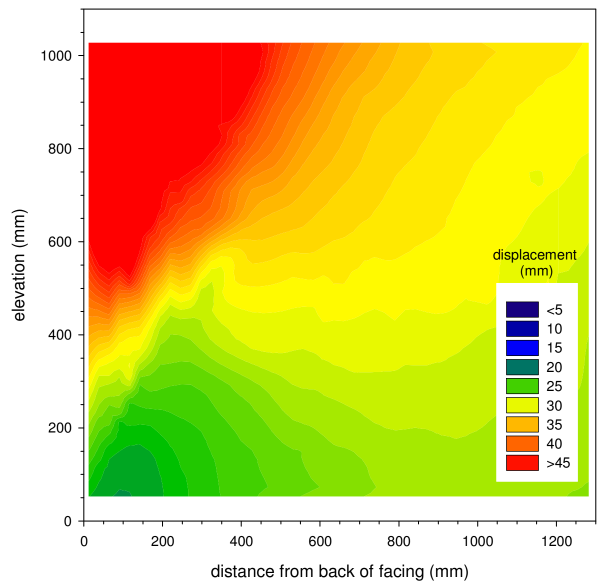

Figure 9. Vertical displacement contours for Wall 17 (compressible base) at q = 66 kPa surcharge.

there was a failure mechanism developed through the soil even though there was no catastrophic collapse of the system. The reason for this is that load was carried by the reinforcement layers and toe of the wall even after the soil had failed. Evidence for this hypothesis is the strain distributions recorded in geogrid reinforcement layers that are superimposed on the contour plots. For Wall 16 (rigid foundation support) the maximum strain in the reinforcement at the onset of soil failure is about 3% (Figure 12). This value agrees well with observations by Allen et al. (2003) from full-scale reinforced (granular) soil walls seated on stiff competent ground that showed that the 3% strain level was also a good indicator of soil failure. In fact, the 3% strain level has been adopted as an ultimate limit state indicator for the internal stability design of reinforced soil walls using the K-stiffness Method (see Allen et al. 2003; Bathurst et al. 2008). Compared to full-scale reinforced walls tests reported by Bathurst et al. (2000) there are no well-defined peaks in the strain profiles that have been associated in this earlier work to one or more internal shear surfaces. However, this is considered to be the result of the reduced-scale of the models in the current study. Figure 13 shows the same comparison for the wall with compressible foundation support. In order to initiate soil failure a lower surcharge pressure is required for this wall and indicator strains for this internal ultimate limit state are typically about 1%. Clearly, the more deformable lower boundary condition for this wall compared to the wall with a stiff foundation base provides less restraint and therefore the soil failure mechanism is developed much earlier in the surcharge loading program. The advantage of the PIV method is that it is possible to detect and locate failure shear bands in the soil as they develop. In previous research by Bathurst and co-workers, the onset of soil failure could only be detected indirectly (e.g. local peaks in strain readings and large increases in toe loads at the wall facing column). Nevertheless, the exact location of initial shear mechanisms in these earlier walls was hard to locate. Only after the tests were taken to large wall displacements and then excavated could internal failure mechanisms be mapped accurately.

6 CONCLUSIONS

Two tests were carried out to investigate the influence of foundation support compressibility on the performance of reduced-scale geosynthetic reinforced soil retaining walls. A large number of contact-type instruments was used to gather performance data for these walls. However, the transparent sides of the strong box that were used to contain the models provided an opportunity to compare measurements and to illustrate the benefits of the PIV technique. This paper shows that:

- PIV measurements and measurements from conventional contact potentiometer devices and manual survey were in general agreement. However, PIV measurements of the wall facing were more accurate than data from manual survey.

- The PIV technique allowed almost continuous displacement and strain fields to be computed. Hence, mechanisms such as the progressive development of internal soil shear bands, down-drag at the connections and soil arching at the base of the soil backfill were clearly visible.

Some of the results presented there have important implications to the design, analysis and performance of geosynthetic reinforced soil walls in the field. Of particular important is the observation that for the wall with a rigid foundation and horizontal toe support, the onset of a contiguous internal soil shear band was consistent with reinforcement strain of about 3%. This is independent

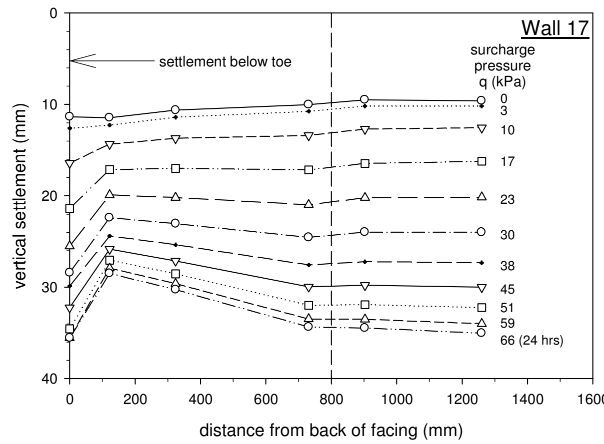

Figure 10. Vertical settlement at base of Wall 17 (compressible base) during surcharging using potentiometer readings.

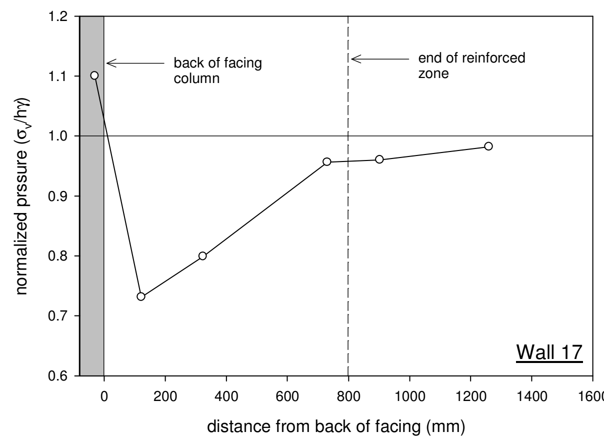

Figure 11. Vertical pressures at base of Wall 17 (compressible foundation) at q = 66 kPa.

corroboration of the K-stiffness method which proposes that 3% strain in the reinforcement be used as an indicator of an ultimate limit state for internal stability of these structures when located on stiff competent foundations.

ACKNOWLEDGEMENTS

Financial support for this study was provided by the Natural Sciences and Engineering Research Council (NSERC) of Canada and grants from the Department of National Defence (Canada).

REFERENCES

Allen, T.M., Bathurst, R.J., Holtz, R.D., Walters, D.L. and Lee, W.F. 2003. A new working stress method for prediction of reinforcement loads in geosynthetic walls. *Canadian Geotechnical Journal*, 40(5): 976-994.

AASHTO 2007. LRFD bridge design specifications. 4th ed. *American Association of State Highway and Transportation Officials (AASHTO*), Washington, D.C.

Bathurst, R.J., Walters, D., Vlachopoulos, N., Burgess, P. G. and Allen, T.M. 2000. Full scale testing of geosynthetic reinforced walls, keynote paper, *ASCE Special Publication No. 103, Advances in Transportation and Geoenvironmental Systems using Geosynthetics, Proceedings of Geo-Denver 2000*, 5-8 August 2000, Denver, Colorado, pp. 201-217.

Bathurst, R.J., Vlachopoulos, N., Walters, D.L., Burgess, P.G. and Allen, T.M. 2006. The influence of facing rigidity on the performance of two geosynthetic reinforced soil retaining walls, *Canadian Geotechnical Journal*, 43(12): 1225-1237.

Bathurst, R. J., Miyata, Y., Nernheim, A. and Allen, A. M. 2008. Refinement of K-stiffness method for geosynthetic-reinforced soil walls, *Geosynthetics International*, 15(4): 269-295.

CFEM 2006. Canadian foundation engineering manual, 4th ed. *Canadian Geotechnical Society*, BiTech Publishers Ltd., Richmond, B.C.

Ezzein, F. 2007. Influence of foundation stiffness on reinforced soil wall behaviour, *Queen's University*, M. Sc. thesis, 446 p.

Ezzein, F. and Bathurst, R.J. 2006. Influence of horizontal toe restraint on reinforced soil retaining wall behaviour, In *CD proceedings of 59th Canadian Geotechnical Conference,* 2006, Vancouver, BC, 8 p.

Ezzein, F. and Bathurst, R.J. 2007. Influence of vertical toe condition on reinforced soil retaining wall behaviour, In *CD proceedings of 60th Canadian Geotechnical Conference,* 2007, Ottawa, ON, 8 p.

Ezzein, F. and Bathurst, R.J. 2008. Influence of foundation compressibility on reinforced soil retaining wall behaviour, In *CD proceedings of 61st Canadian Geotechnical Conference,* 2008, Edmonton, AB, 8 p.

Hatami, K. and Bathurst, R.J. 2005. Development and verification of a numerical model for the analysis of geosynthetic reinforced soil segmental walls under working stress conditions, *Canadian Geotechnical Journal*, 42(4): 1066-1085.

NCMA 1997. Design manual for segmental retaining Walls, 2nd edition, Collin, J., Editor, *National Concrete Masony Association*, Herndon, VA, USA.

Saunders, D.D., Walters, D.L., Bathurst, R.J. and Allen, T.M. 2001. The influence of reinforcement stiffness on the performance of full-scale reinforced soil segmental retaining walls, In *proceedings of 54th Canadian Geotechnical Conference*, 2001, Calgary, AB, Canada, 8 p.

White D.J., Take W.A. and Bolton M.D. 2003. Soil deformation measurement using particle image velocimetry (PIV) and photogrammetry, *Geotechnique* 53(7): 619-631.

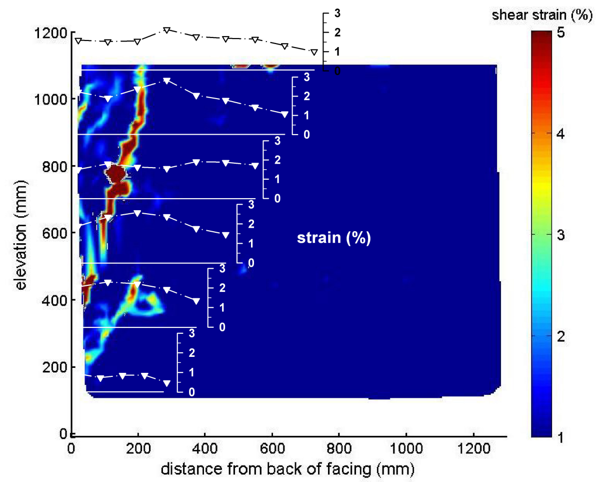

Figure 12. Backfill shear strain contours and reinforcement strain profiles for Wall 16 (rigid foundation) at q = 23 kPa surcharge.

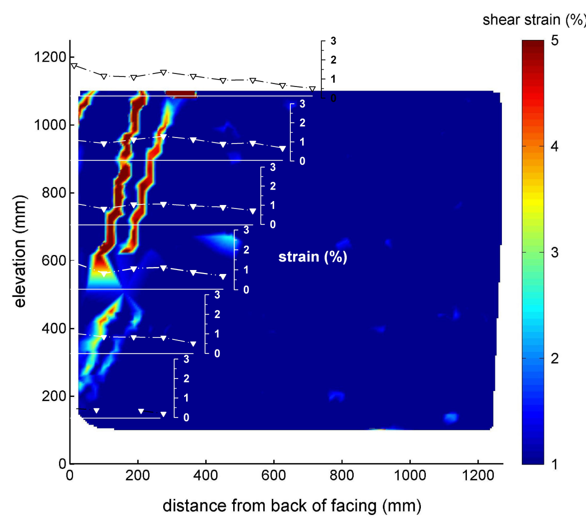

Figure 13. Backfill shear strain contours and reinforcement strain profiles for Wall 17 (compressible foundation) at q = 10 kPa surcharge.